Efficiency measurement of optical components in 45–110 nm range at beamline U27, HLS

Shengnan He (贺胜男), Ying Liu (刘 颖)*, Keqiang Qiu (邱克强), Hongjun Zhou (周洪军), Tonglin Huo (霍同林), and Shaojun Fu (付绍军)

National Synchrotron Radiation Laboratory, University of Science and Technology of China, Hefei 230029, China

**E-mail: liuychch@ustc.edu.cn*

Received May 19, 2010

We propose a general correction method for the efficiency measurement of optical components in the 45–110 nm range to eliminate the contamination of higher-order harmonics at beamline U27 of the Hefei Light Source (HLS). The influence of harmonics can be deducted effectively from the initial measurement results through the analysis of the proportion of harmonics with a transmission grating and the efficiency measurement of optical elements at the harmonics wavelengths. The reflectivity measurement of a gold film is performed at the beamline to verify its validity. Results indicate that the corrected reflectivity is in good agreement with the theoretical value. The maximal deviation amounts to 1.93% at a wavelength of 85 nm and an incident angle of 5°.

OCIS codes: 120.0120, 230.0230.

doi: 10.3788/COL20100812.1131.

The spherical grating monochromator (SGM) branch of beamline U27 at the Hefei Light Source (HLS) is the first and only setup in China that can measure the optical component efficiency in the wavelength range of 5–140 nm[1−4]. However, the SGM output usually contains significant amount of higher-order harmonics that worsens the validity of the measurement dramatically. Harmonics contamination is a common problem of SGMs in synchrotron radiation facilities[5−8], particularly in the 45–110 nm wavelength range because there is no suitable filter that can suppress the higher-order harmonics due to the strong energy absorption characteristics of materials. Neither the differentially pumped absorption gas cell nor multiple mirror reflections[8−10] can be applied in short-term to the beamline U27 due to spatial constraints. Hence, the efficiency measurement of optical components in the 45–110 nm range is still infeasible at this beamline, seriously limiting the corresponding development of domestic research in such spectrum.

To solve the harmonic contamination, we present a correction method of optical component measurement in the vacuum ultraviolet (VUV) spectrum at beamline U27, HLS. The formula derivation of the correction method for typical optical elements is presented. We conduct an experiment measuring gold film reflectivity, and the results indicate that a comparatively accurate measurement can be obtained with the current device using this correction method.

Figure 1 illustrates the layout of the SGM branch equipped with a reflectometer[11,12] located behind the monochromator. Optical elements to be measured are placed on the sample stage. When the incident light intensity $I_0(\lambda)$ contains a large number of higher-order harmonics, the emergent light intensity $I(\lambda)$ of the sample will also contain harmonics. Thus, the proposed measurement procedure involves the following steps: quantitative analysis of the higher-order harmonics using an amplitude transmission grating[13−15], efficiency measurement of optical components at the corresponding harmonic wavelengths, and deduction of harmonic contributions from the original measurement results.

An amplitude transmission grating is employed and installed at normal incidence on the sample stage of the reflectometer. The first-order diffraction angles θ of the fundamental wave and higher-order harmonics can be dispersed by the transmission grating and calculated as

$$d \sin\theta = \lambda/n, \tag{1}$$

where d is the grating period, λ is the fundamental wavelength with $|n|$=1, and λ/n describes the harmonics with $|n|$=2,3,4,$\cdots$.

The first-order diffraction efficiency of the amplitude transmission grating does not change with wavelengths and is described as[16]

$$\eta_{\mathrm{T},1} = \frac{A_{\mathrm{T},1}\,(\lambda/n)}{A_0\,(\lambda/n)} \propto 1/\pi^2, \tag{2}$$

where $A_0(\lambda/n)$ is the n-order harmonic intensity contained in the incident light intensity $I_0(\lambda)$, and $A_{\mathrm{T},1}$ (λ/n) is the first-order diffraction intensity of the n-order harmonic, n=1,2,3,$\cdots$. The subscript "T" denotes transmission. Therefore, the ratio of the n-order harmonic to the fundamental in the incident light, ξ_n (n=2,3,4,$\cdots$), can be calculated by integrating the corresponding diffraction peak:

$$\xi_n = \frac{A_0(\lambda/n)}{A_0(\lambda)} = \frac{A_{\mathrm{T},1}(\lambda/n)}{A_{\mathrm{T},1}(\lambda)}. \tag{3}$$

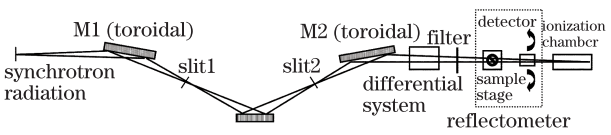

Fig. 1. Sketch of the spherical grating monochromator branch.

Reflection film is selected as an example to expound the correction method. Its reflectivity at the wavelength λ is defined as

$$R(\lambda) = \frac{I(\lambda)}{I_0(\lambda)}, \tag{4}$$

where $I_0(\lambda)$ and $I(\lambda)$ are the intensities of the incident and reflected light, respectively, and they are loch disturbed by harmonics. Hence, Eq. (4) can be resolved as

$$R(\lambda) = \frac{I(\lambda)}{I_0(\lambda)} = \sum_{n=1}^{i} A_n(\lambda/n) \Big/ \sum_{n=1}^{i} A_0(\lambda/n), \tag{5}$$

where $A_n(\lambda/n)$ is the reflected light intensity of the n-order harmonic. It can be decomposed as

$$A_n(\lambda/n) = A_0(\lambda/n) \times R_n(\lambda/n), \tag{6}$$

where $R_n(\lambda/\mathrm{n})$ is the reflectivity of the n-order harmonic that must be measured first to determine the numerator. The harmonics can be suppressed by filters in the 5–45 nm range[3,4]; hence the reflectivity of the n-order harmonics in this band can be measured accurately. Dividing the numerator and the denominator in Eq. (5) by $A_0(\lambda)$, and substituting Eqs. (3) and (6) to Eq. (5) gives

$$R(\lambda) = \frac{R'(\lambda) + \sum_{n=2}^{i} \xi_n \times R_n(\lambda/n)}{1 + \sum_{n=2}^{i} \xi_n}, \tag{7}$$

where $R'(\lambda)=A_1(\lambda)/A_0(\lambda)$ in the numerator is the corrected reflectivity that could be reduced to

$$R'(\lambda) = R(\lambda)\Big(1 + \sum_{n=2}^{i} \xi_n\Big) - \sum_{n=2}^{i} R_n(\lambda/n) \times \xi_n. \tag{8}$$

Equation (8) yields the corrected reflectivity of a reflection film, which is the same as that for the transmission film. However, the reflective and transmissive versions should be treated separately for the characterization of a grating. For the reflection grating, Eq. (8) can be altered as

$$\eta_r'(\lambda) = \eta_r(\lambda)\Big(1 + \sum_{n=2}^{i} \xi_n\Big) - \sum_{n=2}^{i} \eta_{n\times r}(\lambda/n) \times \xi_n, \tag{9}$$

where the footnote r represents the r-order diffraction efficiency and $\eta_{n\times r}(\lambda/\mathrm{n})$ is the $n \times r$-order diffraction efficiency of the n-order harmonic. For the transmission grating, harmonics are dispersed into different directions after diffraction. Therefore, the numerator in Eq. (7) only contains the first factor and the t-order diffraction efficiency of the transmission grating can be corrected as

$$\eta_t'(\lambda) = \eta_t(\lambda)(1 + \sum_{n=2}^{i} \xi_n). \tag{10}$$

To examine this correction method, a 40-nm-thick gold film is prepared through ion beam deposition. Its reflectivity is measured on the U27 beamline in the 5–110–nm band at four incident angles of 5°, 20°, 40°, and 60°. Filters of Si (100 nm), Al (200 nm), and Mg (250 nm) are used to suppress the higher-order contributions in the 12.5–17.5-, 17.5–25.5-, and 25.5–45-nm bands, respectively. Thus, the reflectivity in the 5–45-nm band does not require correction. The direct result of the reflectivity measurement in the 45–55-nm band that is the second-order harmonics of the 90–110-nm is still inaccurate because there is no filter to use. Thus, we first obtain the corrected reflectivity in the 45–55-nm band with the proposed method, which is in good agreement with the calculated reflectivity, then substitute it into Eq. (8) to obtain the accurate reflectivity of the 90–110-nm wavelength region. A slit of 1-mm width is pasted on the detector to improve the resolving power. The theoretical reflectivity of gold is calculated using the IMD film design software[17] and compared with the measured results.

The amplitude transmission grating used in this experiment is gold free-standing with 3300 line/mm and a duty cycle of 1:1 that could suppress even-order diffractions[16]. The thickness of the grating bars is about 300 nm and is absolutely opaque to the radiation when the wavelength is above 8 nm. Thus, the first-order diffraction efficiency is practically independent of the wavelength (Fig. 2). The efficiencies of the higher odd orders decrease as $1/n^2$, where n is the order number[16], then their intensities are too small to be detected in our experiments. Therefore, the harmonics contaminations of the transmission grating can be neglected.

The ratios, ξ_n (n=2,3,4,$\cdots$), as shown in Fig. 3(a) are measured using this transmission grating, which can distinguish harmonic peaks of five orders in the 45–50-nm, six orders in 50–65-nm, and seven orders in 65–110-nm bands. As the wavelength increases, the higher-order diffraction peaks become more complex; they overlap and cannot be distinguished. Both ratios, ξ_n, and their summation increase with the increase in wavelength. The summation of ξ_n reaches up to 22 at the fundamental wavelength of 110 nm, as shown in Fig. 3(b). The quantitative harmonic contributions in Fig. 3 are used to correct the measured reflectivity of gold film according to Eq. (8). In terms of the resolving power of the 3300-line/mm transmission grating, the second factor of Eq. (8) is corrected to the seventh-order. The polarization characteristics of this beamline is indefinitely quantitative, thus the calculated curves under

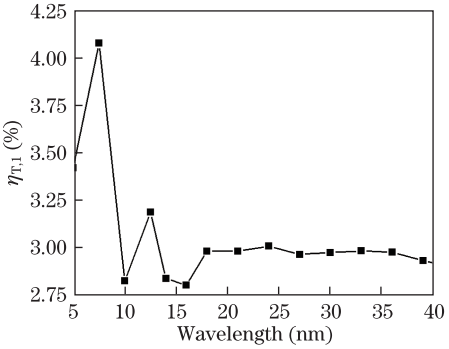

Fig. 2. First-order diffraction efficiency of 3300 line/mm transmission grating in the 5–40–nm band.

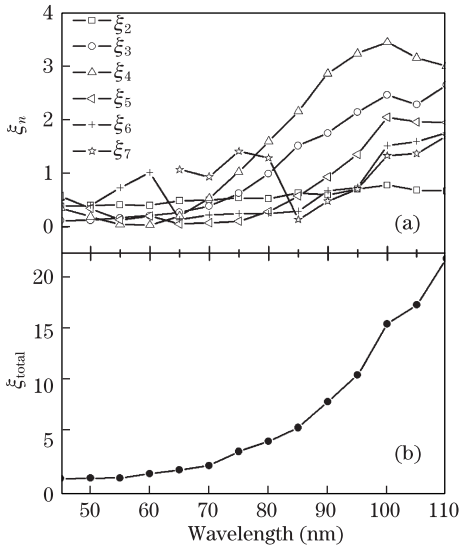

Fig. 3. Intensity ratios of harmonics to fundamental wave measured in 45–110 nm at an interval of 5 nm. (a) Ratios of higher-orders to the first-order, and the absent dots of ratios ξ_5, ξ_6, and ξ_7 are the orders that cannot be distinguished by transmission grating; (b) summed-up ratios of higher-order intensities to the first-order one.

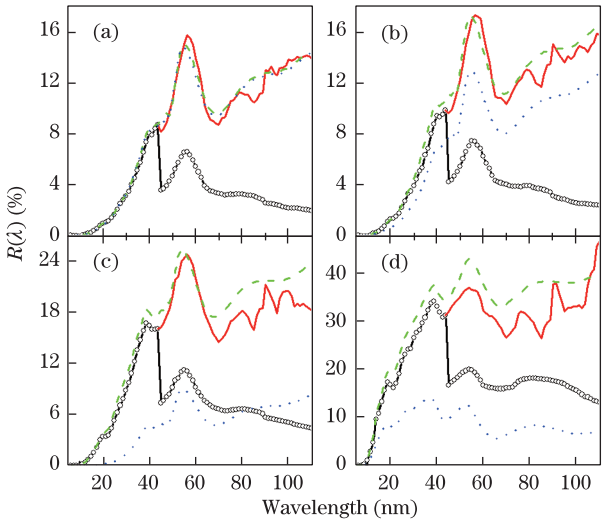

Fig. 4. Calculated, measured, and corrected reflectivities of gold film. The dash curve represents the calculated s-polarization result, the dot curve is the calculated p-polarization result, the curve with circles is the measured result, and the solid curve is the corrected result. (a) At 5° incident angle, (b) at 20° incident angle, (c) at 40° incident angle, (d) at 60° incident angle.

s- and p-polarized conditions are obtained using the IMD film design software[17].

A comparison of the calculated curve with the measured and corrected curves at 5° is shown in Fig. 4(a). At normal incidence, the influence of polarization on reflectivity is negligible. The harmonics could not be suppressed completely by filters in the 5–45-nm band; hence, the measured reflectivities are slightly less than the calculated values. In the 45–110-nm band, the uncorrected measurement data are far less than the calculated curve because of the harmonics contamination. Nevertheless, the corrected curve is in good agreement with the calculated values. The maximal absolute difference between the calculated s-polarized and corrected curves in the 45–110-nm band is 1.93% at the fundamental wavelength of 85 nm.

The same correction is performed for the reflectivity measurement at the incident angles of 20°, 40°, and 60°, as shown in Figs. 4(b)–(d). The results indicate that the deviation between the measured and calculated s-polarized curves in the 5–45-nm band becomes larger with the increasing incident angle. The main reason for these results is that the influence of polarization on the reflectivity becomes more noticeable when the incident angle is close to the Brewster angle. Moreover, the deviation between the corrected and calculated s-polarized curves in the 45–110-nm band is introduced by measurement errors of $R_n(\lambda/n)$ and ξ_n, which become remarkable as the incident angle and wavelength increase. Similar to the incident angle of 60° that is close to the grazing angle, as shown in Fig. 4(d), the reflectivity at shorter wavelengths is still considerable; thus, the harmonic contributions mixed in the reflection light are significant, and the higher-order factors ξ_n, of which the subscript n is greater than 7 in Eq. (3), cannot be omitted as a small quantity. These results lead to the larger corrected values in the long wavelength band.

In conclusion, this correction method based on the amplitude transmission grating can be applied effectively to the optical component measurement near normal incidence. The accuracy of this correction degrades when the measurement is executed at grazing incidence. The correction results compared with the calculated results indicate that the synchrotron source is not entirely s-polarized light. The correction accuracy could be improved if the polarization degree of the synchrotron radiation source is determined quantitatively, as well as through the use of a transmission grating with higher density or by increasing the distance between the sample and detector to distinguish more higher-order harmonics. This method can be extended for applications at other synchrotron radiation beamlines with similar problems.

This work was supported by the National Natural Science Foundation of China under Grant No. 10975139. The authors are greatly indebted to Christoph Braig from Friedrich Schiller University Jena for his advice and assistance in this manuscript.

References

1. H. Zhou, T. Huo, P. Zhong, G. Zhang, and J. Zheng, J. University of Science and Technology of China (in Chinese) **37,** 402 (2007).
2. S. Gan, Z. Liu, B. Sheng, X. Xu, Y. Hong, Y. Liu, H. Zhou, T. Huo, and S. Fu, Acta Opt. Sin. (in Chinese) **28,** 2036 (2008).
3. L. Bai, J. Zhu, J. Xu, Q. Huang, W. Wu, X. Wang, Z. Wang, and L. Chen, Acta Opt. Sin. (in Chinese) **29,** 2615 (2009).
4. H. Lin, L. Zhang, C. Jin, H. Zhou, and T. Huo, Chin. Opt. Lett. **7,** 180 (2009).
5. H. Zhou, P. Zhong, T. Huo, J. Zheng, G. Zhang, and Z. Qi, Opt. Precision Eng. (in Chinese) **15,** 1915 (2007).
6. H. Zhou, P. Zhong, T. Huo, J. Zheng, G. Zhang, and Z. Qi, Opt. Precision Eng. (in Chinese) **15,** 1016 (2007).

7. R. L. C. Filho, M. G. P. Homem, R. Landers, and A. N. de Brito, J. Electron. Spectrosc. Relat. Phenom. **144-147,** 1125 (2005).
8. A. G. Suits, P. Helmann, X. Yang, M. Evans, C.-W. Hsu, K. Lu, and Y. T. Lee, Rev. Sci. Instrum. **66,** 4841 (1995).
9. B. Mercier, M. Compin, C. Prevost, G. Bellec, R. Thissen, O. Dutuit, and L. Nahon, J. Vac. Sci. Technol. A **18,** 2533 (2000).
10. S. N. He, Y. Liu, H. J. Zhou, T. L. Huo, and S. J. Fu, Nuclear Techniques (in Chinese) **32,** 409 (2009).
11. S. Xue, J. Shao, Q. Lu, Z. Wang, and Z. Xu, Opt. Precision Eng. (in Chinese) **12,** 480 (2004).
12. S. Gan, Z. Liu, X. Xu, Y. Hong, Y. Liu, H. Zhou, T. Huo, and S. Fu, Acta Opt. Sin. (in Chinese) **28,** 2136 (2008).
13. M. Kühne and P. Müller, Rev. Sci. Instrum. **60,** 2101 (1989).
14. H. Zhou, J. Zheng, T. Huo, G. Zhang, Z. Qi, and P. Zhong, Opt. Precision Eng. (in Chinese) **15,** 640 (2007).
15. K. Sun, J. Zhang, M. Cui, G. Yang, S. Jiang, R. Yi, W. Zhang, and Y. Cui, High Power Laser and Particle Beams (in Chinese) **19,** 1308 (2007).
16. T. H. Markert, D. Dewey, J. E. Davis, K. A. Flanagan, D. E. Graessle, J. M. Bauer, and C. S. Nelson, Proc. SPIE **2518,** 424 (1995).
17. D. L. Windt, Computers in Physics **12,** 360 (1998).